

NONLINEAR MODEL-BASED ADAPTIVE CONTROL OF A SOLENOID-VALVE SYSTEM

**DongBin Lee, C. Nataraj,
and Peiman Naseradinmousavi**
Department of Mechanical Engineering
Center for Nonlinear Dynamics and Control
(CENDAC)
Villanova University, Villanova, PA 19085
dongbin.lee-, c.nataraj-, pnaser01@villanova.edu

ABSTRACT

In this paper, a model-based control algorithm is developed for a solenoid-valve system. Solenoids and butterfly valves have uncertainties in multiple parameters in the model, which make the system difficult to adjust to the environment. These are further complicated by combining the solenoid and butterfly dynamic models. The control objective of a solenoid-valve system is to position the angle of the butterfly valve through the electric-driven actuator in spite of the complexity presented by uncertainties. The novelty of the controller design is that the current source of the solenoid valve from the model of the electromagnetic force is substituted for the control input in order to reach the set-point of the butterfly disk based on the error signals, overcoming the uncertainties represented by lumped parameters groups, and a stable controller is designed via the Lyapunov-based approach for the stability of the system and obtaining the control objective. The parameter groups are updated by adaptation laws using a projection algorithm. Numerical simulation is shown to demonstrate good performance of the proposed approach.

NOMENCLATURE

J	= the inertia moment [kgm^2]
r_g	= the radius of pinion gear [m]
m	= the mass of solenoid plunger [kg]
B_1, B_2	= the damping coefficients of the solenoid and butterfly valve [Ns/m], respectively
k	= the spring stiffness [N/m]
N	= number of turns of the coil
R	= the resistance of the coil [Ω]
F_{mag}	= the magnetic force [N]
F_c	= the contact force [N] (or the resultant force F_r).
$T_c(\alpha)$	= the hydrodynamic torque coefficient

T_h, T_b = hydrodynamic and bearing torques, respectively.

$\frac{V_J}{V_O}(\alpha)$ = the ratio of the jet and the mean flow velocity

ρ = the flow density [kg / m^3]

D_s = stem diameter

D_p = the pipe diameter [m]

ΔP_v = differential valve pressure

$C_R(\alpha)$ = bearing torque coefficient

INTRODUCTION

In order to achieve advanced automation in such systems as marine vessels, or ship-based machinery system, solenoid actuators and valves are often used because they are a critical part of the automation system which increases survivability and capability. The electric-driven solenoid-valve system and its sophisticated control can provide high levels of automation on large systems. The useful function of the solenoid-valve, once an electrical signal (current or voltage) is applied, is to activate a mechanical motion such as displacement or rotation via the solenoid magnetic forces and torques [4]. The proportional solenoids normally require integrated electronics for position sensing in order to compensate for mechanical motion and nonlinearities like magnetic hysteresis [7]. Hydrodynamic torque of a butterfly valve is core knowledge of fluid valve system design [5] and it is known that most of the valves in real system have strongly nonlinear characteristics between the force and displacement [1].

The use of an intelligent approach such as robust, adaptive, or optimal control of the actuator-valve machinery systems will benefit a wide spectrum of nonlinear systems. This approach will not only decrease the amount of costs and casualties, but also will increase the performance of the

mechatronics system. To investigate the particular application, it is important to emphasize the nonlinear dynamic modeling, design and analysis, and control of such actuator-valve systems, because the accuracy and reliability of these systems depend highly on the mathematical system modeling and its validation. In [3], the authors developed and analyzed the nonlinear dynamic model of a solenoid-valve system.

This paper will focus on model-based nonlinear adaptive control of an actuator-butterfly valve. The solenoid-valve system is described based on exact model knowledge of the system. Figure 1 shows the integrated system, which consists of an electric-driven solenoid and a butterfly valve. The valve operates by solenoids which use magnetic coil to move a solenoid movable plunger connected with the valve stem by means of a gear train and linkage. The control input is designed by substituting the current signal from the model of the electromagnetic force, pulling the plunger, and then controlling the angular position of the butterfly valve. The system has uncertainties in multiple parameters in the dynamic model, which requests the system to continuously adjust to the environment and consequently requires adaptation for sustainability and capability. The integrated system is highly nonlinear in addition to its parameter uncertainties. Hence, an adaptive control method is proposed [6] and error signals of the set-point trajectory tracking are developed for the solenoid-valve system. A closed-loop stable controller is designed by introducing a Lyapunov-type stability analysis [8] based on the above error dynamics of the nonlinear solenoid-valve system, which yields a stable system. The numerical results in the simulation, which use the exact same controller design, show initial verification. Therefore simulation results showed "perfect" performance. Unless we use more sophisticated/accurate simulation model, or hardware in the loop simulation, simulation results don't mean anything.

MODEL-BASED NONLINEAR SYSTEM

System Model

The dynamic equations of motion of the plunger and butterfly valve are given by [3]

$$\begin{aligned} m\ddot{x} + B_1\dot{x} + kx &= F_{mag} - F_c, \\ J\ddot{\alpha} + B_2\dot{\alpha} &= r_g F_c - T_{tot} \end{aligned} \quad (1)$$

where $x(t)$ is the displacement of the solenoid plunger and $\alpha(t)$ is the closing angle of butterfly disk. Total torque T_{tot} is the sum of the hydrodynamic and bearing torques expressed as

$$T_{tot} = T_h + T_b.$$

The hydrodynamic torque is obtained by reviewing three-dimensional hydrodynamic torque coefficient based on [1], [2] as

$$T_h = \frac{8}{3\pi} \rho D_p^2 V_o^2 T_c(\alpha) \left[\frac{V_J}{V_o}(\alpha) \right]^2$$

where, both $T_c(\alpha)$ and $\left[\frac{V_J}{V_o}(\alpha) \right]$ depend on the

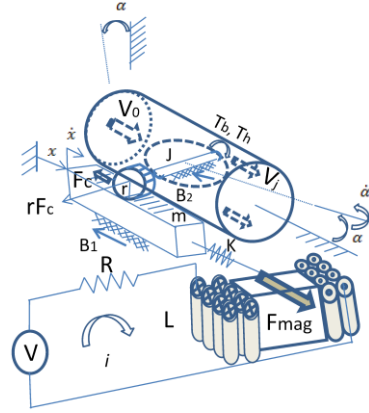


FIGURE 1. SYSTEM CONFIGURATION

closing angle (α) of the butterfly valve. For the bearing torque, $T_b = \frac{\pi}{8} \mu D_s D_p^2 \Delta P_v C_R(\alpha)$ (see [3] for the torque coefficients). Solving the two equations in (1) with F_c and substituting the magnetic force, F_{mag} , into the equation yields

$$\begin{aligned} \left(m + \frac{J}{r_g^2} \right) r_g \ddot{x} + \left(B_1 + \frac{B_2}{r_g^2} \right) r_g \dot{x} + k r_g x \\ = r_g \frac{C_2 N^2}{2(C_1 + C_2 x)^2} i^2 - T_{tot} \end{aligned} \quad (2)$$

where the current rate of the solenoid actuator model, $\frac{di}{dt} = \frac{(V_s - Ri)(C_1 + C_2 x)}{N^2} + \frac{C_2 \dot{x}}{(C_1 + C_2 x)} i$ is given in [3] and C_1 and C_2 are obtained from [4]. For the subsequent controller design, the current source $i^2(t)$ is substituted for the system control input $u(t)$, then the following equation is obtained:

$$\begin{aligned} \left(m + \frac{J}{r_g^2} \right) r_g \ddot{x} + \left(B_1 + \frac{B_2}{r_g^2} \right) r_g \dot{x} + k r_g x \\ = r_g \frac{C_2 N^2}{2(C_1 + C_2 x)^2} u - T_{tot} \end{aligned} \quad (3)$$

Multiplying eq. (3) with the inverse term of the control input, $\frac{2(C_1 + C_2 x)^2}{r_g C_2 N^2}$, yields a compact form of dynamic equation as

$$M(x, \theta) \ddot{x} + C(x, \theta) \dot{x} + D(x, \theta) x = u - B(x, \theta) (T_h + T_b) \quad (4)$$

where lumped expression of the combined parameters are based on θ due to their combination in the developed system matrices. $\theta = [\theta_1, \theta_2, \dots, \theta_i, \dots, \theta_n]$, in which θ_i is i_{th}

parameter value as shown in the Table 1 and the matrices are defined as follows.

$$M(x, \theta) = \left(m + \frac{J}{r_g^2} \right) r_g B(x, \theta), \quad B(x, \theta) = \frac{2(C_1 + C_2 x)^2}{r_g C_2 N^2}$$

$$C(x, \theta) = \left(B_1 + \frac{B_2}{r_g^2} \right) r_g B(x, \theta), \quad D(x, \theta) = k r_g B(x, \theta).$$

Error Signals

The following set-point control approach is used. Let $x_d(t)$ define the set-point trajectory and then the error can be defined as

$$e \equiv x_d - x, \quad \dot{e} \equiv \dot{x}_d - \dot{x}, \quad \ddot{e} \equiv \ddot{x}_d - \ddot{x} \quad (5)$$

where $\dot{x}_d(t)$ and $\ddot{x}_d(t)$ are the first and second time derivatives of x_d , and which are assumed to be bounded. Pre-multiplying $\ddot{e}(t)$ in the last error signal of (5) with $M(x, \theta)$ yields

$$M(x, \theta) \ddot{e} = M(x, \theta) \ddot{x}_d - M(x, \theta) \ddot{x}$$

Substituting $M(x, \theta)$ in (4) into the above equation produces

$$M(x, \theta) \ddot{e} = M(x, \theta) \ddot{x}_d + C(x, \theta) \dot{x} + D(x, \theta) x - u + B(x, \theta)(T_h + T_b) \quad (6)$$

We define the filtered error signals as

$$r \equiv \dot{e} + e. \quad (7)$$

Then the time derivative of $r(t)$ is

$$\dot{r} \equiv \ddot{e} + \dot{e}. \quad (8)$$

Multiplying (8) with $M(x, \theta)$ and then substituting for $M(x, \theta) \ddot{e}(t)$ in (6) yields

$$M(x, \theta) \dot{r} = M(x, \theta) \ddot{x}_d + C(x, \theta) \dot{x} + D(x, \theta) x - u + B(x, \theta)(T_h + T_b) + M(x, \theta) \dot{e} + \frac{1}{r_g^2} e - \frac{1}{r_g^2} e \quad (9)$$

where $\frac{1}{r_g^2} e(t)$ is added and subtracted for further development of the control design based on Lyapunov's method.

Adaptive Feedback Control

Let $V(t)$ be a Lyapunov candidate function

$$V = \frac{1}{2} \left(r^T M r + e^T e + e_\alpha^T e_\alpha + \tilde{\Theta}^T \Gamma^{-1} \tilde{\Theta} \right) \quad (10)$$

where the last term of the Lyapunov candidate function, $\Gamma = \gamma I_{ppp}$ is a constant diagonal matrix with the gain value γ , I_{ppp} is a ppp identity matrix, and the parameter estimation error, $\tilde{\Theta}$, is defined as $\tilde{\Theta} = \Theta - \hat{\Theta}$ where $\Theta \in \mathfrak{R}^p$ is a known constant parameter vector and $\hat{\Theta} \in \mathfrak{R}^p$ is the estimated

constant parameter vector (see TABLE 4 in ANNEX A). Differentiating (10) yields

$$\dot{V} = r^T \dot{M} r + \frac{1}{2} r^T \dot{M} r + e^T \dot{e} + \frac{1}{r_g^2} e^T \dot{e} - \tilde{\Theta}^T \Gamma^{-1} \dot{\tilde{\Theta}} \quad (11)$$

where the time derivative of the inertia matrix is obtained as

$$\dot{M}(x, \theta) = \left(m + \frac{J}{r_g^2} \right) r_g \frac{d}{dx} B(x, \theta)$$

$$= \left(m + \frac{J}{r_g^2} \right) \frac{4(C_1 + C_2 x)}{N^2} \dot{x},$$

and $e_\alpha^T \dot{e}_\alpha = \frac{1}{r_g^2} e^T \dot{e}$ as

$$e_\alpha \equiv \alpha_d - \alpha = \frac{x_d}{r_g} - \frac{x}{r_g} = \frac{e}{r_g}, \quad \dot{e}_\alpha \equiv \dot{\alpha}_d - \dot{\alpha} = \frac{\dot{x}_d}{r_g} - \frac{\dot{x}}{r_g} = \frac{\dot{e}}{r_g},$$

in which the error signals of the valve angle, $e_\alpha(t)$, can be defined using the geometric relationship and $\tilde{\Theta} = -\hat{\Theta}$ comes from the definition of $\tilde{\Theta}$. Substituting $M(x, \theta) \dot{r}(t)$ into (11) yields

$$\dot{V} = r^T \left(M \dot{x}_d + C \dot{x} + D x - u + B(T_h + T_b) + M \dot{e} + \frac{1}{r_g^2} e \right) - \frac{(\dot{e} + e)^T e}{r_g^2} + \frac{1}{2} r^T \dot{M} r + e^T \dot{e} + \frac{1}{r_g^2} e^T \dot{e} - \tilde{\Theta}^T \Gamma^{-1} \dot{\tilde{\Theta}} \quad (12)$$

where the definition of $r(t)$ in (7) is used in the second row, its first term $\frac{1}{r_g^2} e^T \dot{e}$ is required to cancel the last second term

having the opposite sign because they are scalar since

$$\dot{e}^T e = e^T \dot{e}.$$

Then, combining the parameterizable terms produces

$$\dot{V} = r^T (W \Theta - u) - \frac{e^T e}{r_g^2} + e^T \dot{e} - \tilde{\Theta}^T \Gamma^{-1} \dot{\tilde{\Theta}} \quad (13)$$

where the term, $W \Theta \in \mathfrak{R}^n$, is defined as

$$W \Theta \equiv M \dot{x}_d + C \dot{x} + D x + B(T_h + T_b) + M \dot{e} + \frac{1}{r_g^2} e + \frac{1}{2} \dot{M} r, \quad (14)$$

and $W(\dot{x}_d, \dot{x}, x, r, \alpha, \dot{e}, e) \in \mathfrak{R}^{n \times p}$ is a regression term.

The control input can be designed, yielding \dot{V} to satisfy negative definiteness (to be shown later) as

$$u = W \hat{\Theta} + k_1 r + e \quad (15)$$

where $r(t)$ is a feedback error term in which k_1 is a positive constant as the control gain, $e(t)$ is added to cancel the term outside the parenthesis after premultiplying by $r(t)$, and $W \hat{\Theta}$ is defined as

$$W\hat{\Theta} = \hat{M}\ddot{x}_d + \hat{C}\dot{x} + \hat{D}x + \hat{B}(\hat{T}_h + \hat{T}_b) + \hat{M}\dot{e} + \frac{1}{\hat{r}_g^2}e + \frac{1}{2}\hat{M}r \quad (16)$$

and the estimated parameter sets are given

$$\hat{M}(x, \theta) = \hat{M}_s \hat{B}(x, \theta) \quad \text{where } \hat{M}_s = \left(\hat{m} + \frac{\hat{J}}{\hat{r}_g^2}\right)$$

$$\hat{C}(x, \theta) = \hat{C}_s \hat{B}(x, \theta) \quad \text{where } \hat{C}_s = \left(\hat{B}_1 + \frac{\hat{B}_2}{\hat{r}_g^2}\right), \text{ and}$$

$$\hat{D}(x, \theta) = \hat{k}_g \hat{B}(x, \theta) \quad \text{where } \hat{B}(x, \theta) = \frac{2(\hat{C}_1 + \hat{C}_2 x)^2}{\hat{r}_g C_2 \hat{N}^2}.$$

Substituting u in (15) into \dot{V} in (13) yields

$$\begin{aligned} \dot{V} &= r^T W\tilde{\Theta} - r^T k_1 r - (\dot{e} + e)^T e - \frac{e^T e}{r_g^2} + e^T \dot{e} - \tilde{\Theta}^T \Gamma^{-1} \dot{\hat{\Theta}} \\ &= -r^T k_1 r - \left(1 + \frac{1}{r_g^2}\right) e^T e + \tilde{\Theta}^T \left\{W^T r - \Gamma^{-1} \dot{\hat{\Theta}}\right\}. \end{aligned} \quad (17)$$

where $W\tilde{\Theta}$ is defined as

$$\begin{aligned} W\tilde{\Theta} &= (M - \hat{M})(\ddot{x}_d + \dot{e}) + (C - \hat{C})\dot{x} + (D - \hat{D})x + \\ &\quad \left(BT_{tot} - \hat{B}\hat{T}_{tot}\right) + \left(\frac{1}{r_g^2} - \frac{1}{\hat{r}_g^2}\right)e + \frac{1}{2}(M - \hat{M})r, \end{aligned}$$

which yields

$$\begin{aligned} W\tilde{\Theta} &= \tilde{M}(\ddot{x}_d + \dot{e}) + \tilde{C}\dot{x} + \tilde{D}x + \tilde{B}\tilde{T}_{hl}T_c(\alpha)\frac{V_J}{V_O}(\alpha) + \\ &\quad \tilde{B}\tilde{T}_{bl}C_R(\alpha) + \tilde{r}_g e + \frac{1}{2}\tilde{M}r \end{aligned} \quad (18)$$

where

$$\begin{aligned} \tilde{M} &= M - \hat{M}, \quad \tilde{C} = C - \hat{C}, \quad \tilde{D} = D - \hat{D}, \quad \tilde{B}\tilde{T}_{hl} = BT_{hl} - \hat{B}\hat{T}_{hl}, \\ \tilde{B}\tilde{T}_{bl} &= BT_{bl} - \hat{B}\hat{T}_{bl}, \quad \tilde{r}_g = \frac{1}{r_g^2} - \frac{1}{\hat{r}_g^2}, \quad \text{and } \tilde{M} = M - \hat{M} \end{aligned}$$

in which

$$\hat{T}_{hl} = \frac{8}{3\pi}(\hat{\rho}\hat{D}_p^2\hat{V}_O^2) \text{ and } \hat{T}_{bl} = \frac{\pi}{8}\hat{\mu}\hat{D}_s\hat{D}_p^2\Delta\hat{P}_v.$$

Owing to the subsequent adaptation law, the time derivative of $V(t)$ yields the following upper bound as

$$\dot{V} \leq -k_1 \|r\|^2 - \left(1 + \frac{1}{r_g^2}\right) \|e\|^2, \quad (22)$$

which can be written as

$$\dot{V} \leq -k_2 \|z\|^2 \quad (23)$$

where k_2 is a positive constant and

$$z = [r, e]^T$$

and

$$k_2 = \min\left\{k_1, \left(1 + \frac{1}{r_g^2}\right)\right\}$$

Remark The control law of (15) ensures the set-point error is bounded. Therefore, according to the analysis from (11) to (23) and the property of $V(t)$ and $\dot{V}(t)$, it is straightforward to make a conclusion that $z(t)$ is bounded. Thus, $r(t)$, $e(t)$, and then $e_\alpha(t)$ are bounded. Also $\tilde{\Theta}$ is bounded due to the projection method and the constant known parameter of Θ . Owing to the bounds of $r(t)$, $e(t)$ in (7), $\dot{e}(t)$ is bounded. Note that all desired trajectories are assumed to be bounded. Thus, $x(t)$ and $\dot{x}(t)$ are bounded due to the bounded trajectories of $x_d(t)$ and $\dot{x}_d(t)$. Thus, M , B , C , and D matrices in (4) are bounded because Θ , $x(t)$ are bounded, and also \dot{B} and \dot{M} are bounded in (11) owing to the bounds of $\dot{x}(t)$. T_{tot} is bounded because $\alpha(t)$ is bounded. Thus, the control input $u(t)$ is bounded due to the boundedness of Θ . This leads the boundedness of $\ddot{x}(t)$ in the dynamic model eq. (4) which also enables the boundedness of $\ddot{e}(t)$ in (5) and then, the set-point tracking error $\dot{r}(t)$ in (8) is bounded. Therefore, we can conclude that all signals are bounded.

Adaptation Laws for Parameter Updates

The following is assumed to define the upper and lower bounds of each unknown parameters

$$\underline{\hat{\Theta}}_j \leq \hat{\Theta}_j \leq \bar{\hat{\Theta}}_j \quad (19)$$

where $\hat{\Theta}_j$ is the estimated constant parameters, $\underline{\hat{\Theta}}_j$, $\bar{\hat{\Theta}}_j$ are unknown lower and upper bounds of the estimated parameters as shown in system parameters, respectively, which will be set to the amount of percentage of their true values. $\hat{\Theta}_j$ vector is designed to update using a projection-based algorithm as follows

$$\dot{\hat{\Theta}}_j = \text{Proj}\left\{\Gamma W^T r, \hat{\Theta}_j\right\} \quad (20)$$

where $\text{Proj}\{\cdot\}$ is the projection operator [6] and each parameter is adaptively updated using adaptation laws for online estimation of unknown parameter as follows:

$$\text{Proj}\left\{\dot{\hat{\Theta}}_j\right\} = \text{Proj}\left\{\Gamma W^T r, \hat{\Theta}_j\right\}$$

$$= \begin{cases} \Gamma W^T r & \text{if } \hat{\Theta}_j > \bar{\hat{\Theta}}_j \text{ and } \hat{\Theta}_j < \underline{\hat{\Theta}}_j \\ \Gamma W^T r & \text{if } \hat{\Theta}_j = \bar{\hat{\Theta}}_j \text{ and if } \Gamma W^T r > 0 \\ \Gamma W^T r & \text{if } \hat{\Theta}_j = \underline{\hat{\Theta}}_j \text{ and if } \Gamma W^T r \leq 0 \\ 0 & \text{elsewhere} \end{cases} \quad (21)$$

SIMULATION RESULTS

Based on the dynamic model in (4), a typical parameter set for this simulation is given by

TABLE 1. THE LIST OF SIMULATION PARAMETERS

m	J	r_g	B_1	B_2	k	N	R
0.1	$1.04e^{-6}$	$1e^{-2}$	10	20	$4e^2$	$8.8e^3$	1.0
C_1	C_2	ρ	D_p	V_O	μ	D_s	ΔP_v
$1.57e^6$	$6.32e^8$	$1e^3$	6.0	3.7	0.1	0.1	0.5

Numerical simulation is performed to verify the proposed controllers with changing parameter values as shown in the table. Among the parameter values it can be divided into two categories; operational values such as D_p and V_O and uncertain values like damping coefficients such as B_1 , B_2 , and μ . One of the operational parameter values are evaluated in this simulation where the pipe diameter D_p shown in TABLE 1 is used to vary from 5 inches to 9 inches as follows:

$$D_p = \{5.0, 6.0, 7.0, 8.0, 9.0\},$$

and the simulation results are provided here. More simulation results will be provided later for the responses of other parameters. The amount of variation of the unknown parameter sets, the upper and lower bounds, in the adaptive control method is 90% of their real values. The real values of the hydrodynamic torque coefficient and the ratio of the jet and flow velocities for the simulation are given as look-up tables which are borrowed from [2]. In TABLE 2 the desired set-point distances of the solenoid are given as

TABLE 2. THE LIST OF DESIRED TRAJECTORIES

	x_d	α°
Group 1	$A_1 B(1 - e^{-Bt})$	85
Group 2	$A_2 B(1 - e^{-Bt})$	82
Group 3	$A_3 B(1 - e^{-Bt})$	81
Group 4	$A_4 B(1 - e^{-Bt})$	80
Group 5	$A_5 B(1 - e^{-Bt})$	75

where $A_1 = 0.0148$, $A_2 = 0.0143$, $A_3 = 0.0141$, $A_4 = 0.0140$, $A_5 = 0.0134$ and $B = 5$. The control gains were chosen selectively as $\gamma = 50$, $k_1 = 0.01$ for all cases.

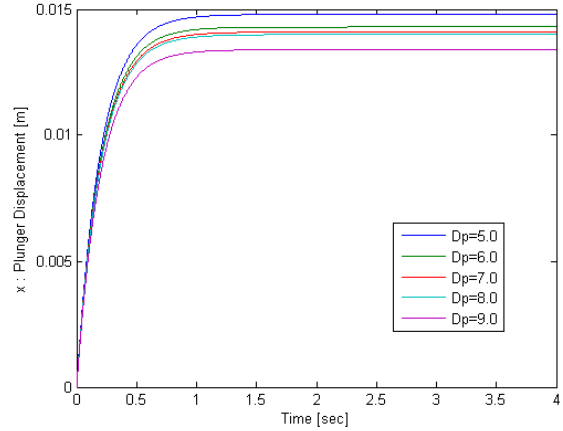


FIGURE 2. PLUNGER DISPLACEMENT

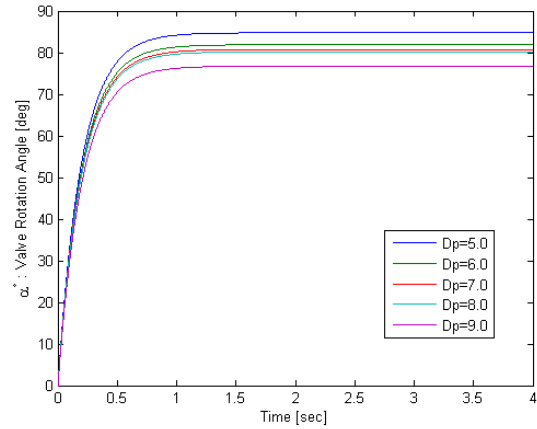


FIGURE 3. VALVE ROTATION ANGLE

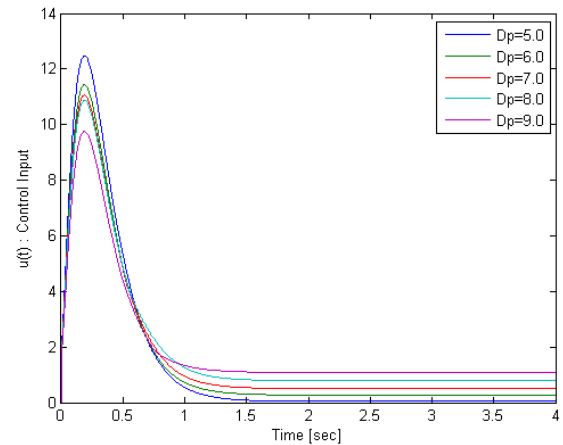


FIGURE 4. CONTROL INPUT

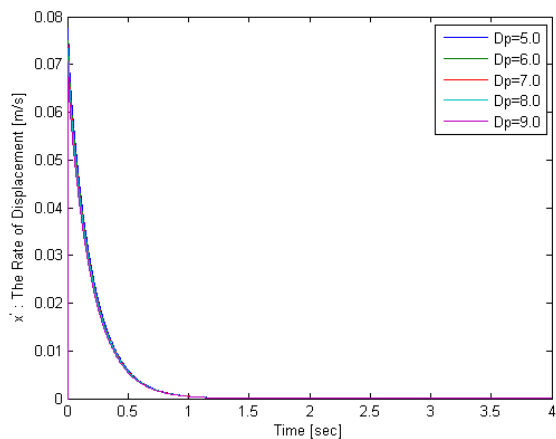


FIGURE 5. THE RATE OF PLUNGER DISPLACEMENT

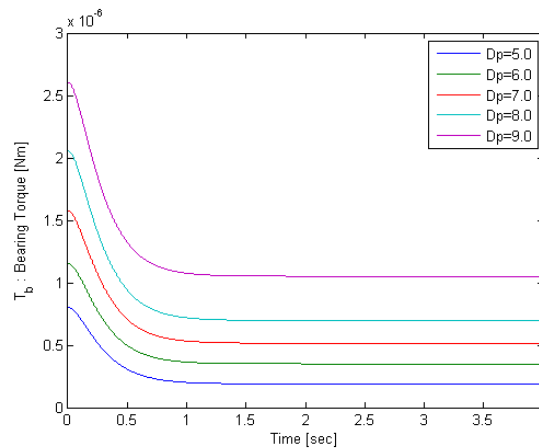


FIGURE 8. BEARING TORQUE

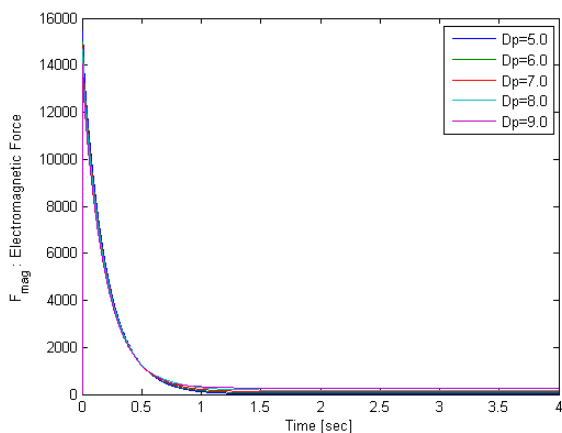


FIGURE 6. ELECTROMAGNETIC FORCE

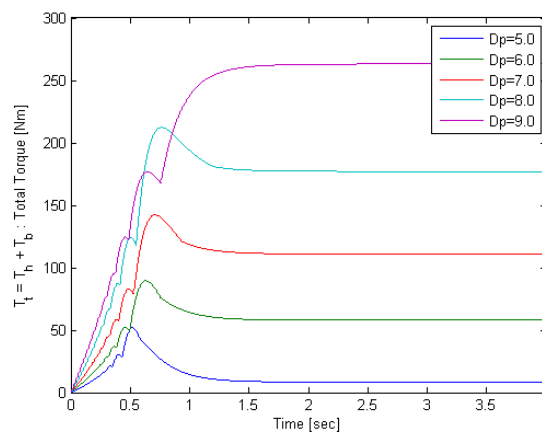


FIGURE 9. THE TOTAL TORQUE

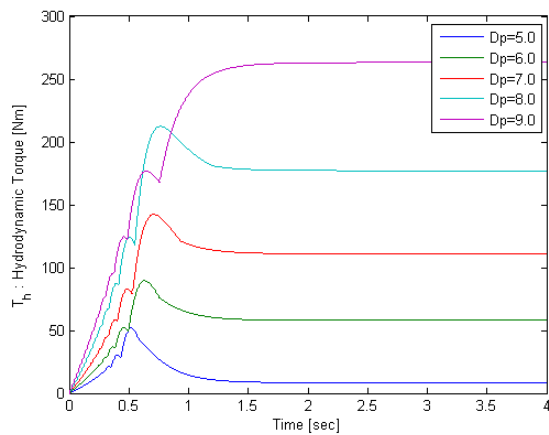


FIGURE 7. HYDRODYNAMIC TORQUE

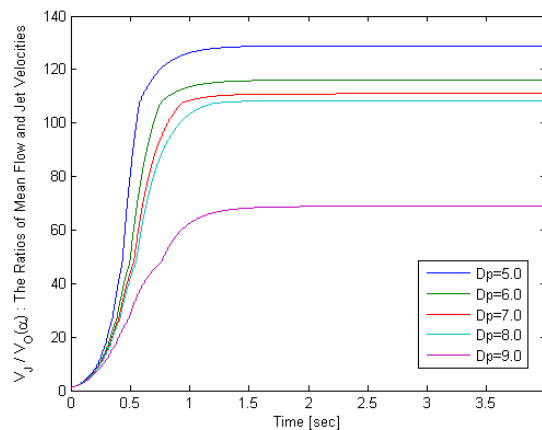


FIGURE 10. THE RATIO OF VJ/V0

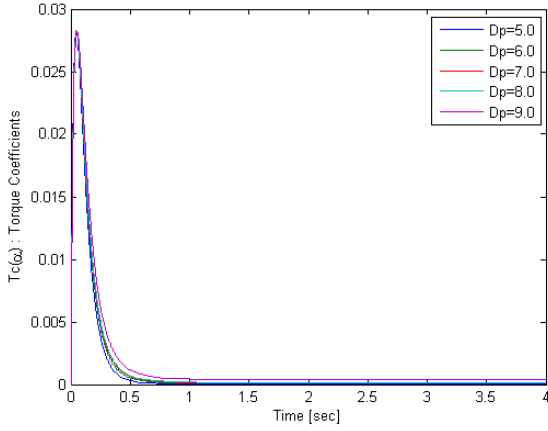


FIGURE 11. HYDRODYNAMIC TORQUE COEFFICIENTS

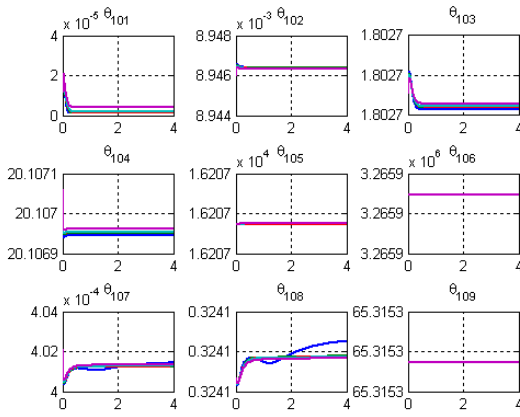


FIGURE 12. PARAMETER ESTIMATES: $\hat{\theta}_{101} \sim \hat{\theta}_{109}$

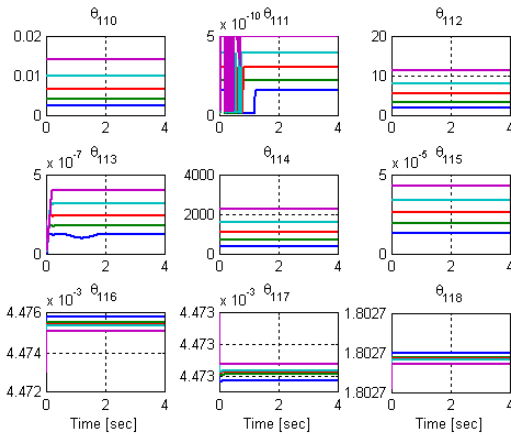


FIGURE 13. PARAMETER ESTIMATES: $\hat{\theta}_{110} \sim \hat{\theta}_{119}$

the above adaptive control approach shows better results.

The above adaptive control approach shows better results compared to the simulation results obtained from [3] using non-adaptive method which are shown in Figure 14 and Figure 15,

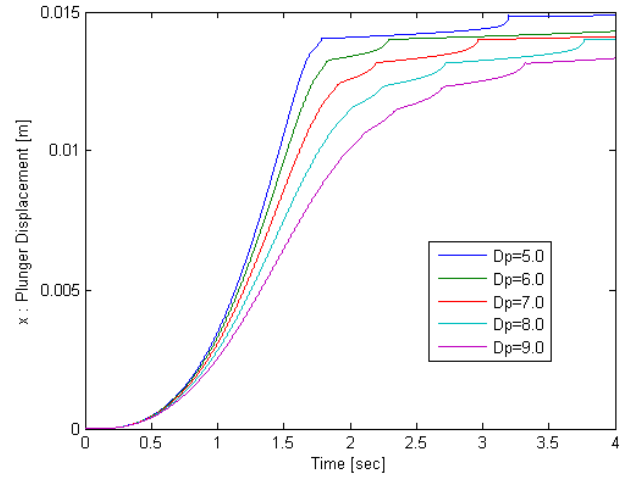


FIGURE 14. PLUNGER DISPLACEMENT (non-adaptive)

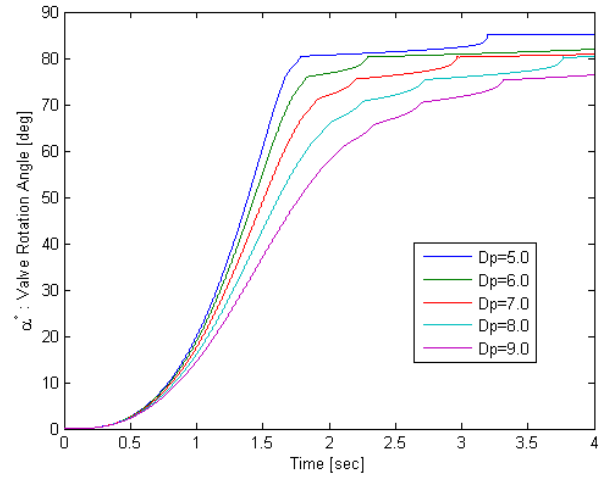


FIGURE 15. VALVE ROTATION ANGLE (non-adaptive)

CONCLUSION

Based on the nonlinear dynamic model of a typical solenoid-valve system, an adaptive control approach is developed accounting for uncertainties in multiple parameters. The parameter estimation for the unknown bounded parameters is performed using a projection algorithm. A stable adaptive control approach is designed by introducing Lyapunov-type stability while obtaining the set-point control. Numerical simulation is demonstrated to verify the initial performance of the proposed approach. Thus, when compared to the non-adaptive method showing nonlinear phenomena, the responses of the plunger displacement and the valve rotating angle are quicker and smoother. Future work will be focused on illustrating the results in experiments or hardware in the loop.

APPENDIX A

Briefly introducing $W\hat{\Theta}$ in (16) as follows:

TABLE 3. REGRESSION TERMS

No.	Terms	No.	Terms
W_{101}	\ddot{x}_d	W_{110}	$T_c(\alpha) \left[\frac{V_J}{V_O}(\alpha) \right]^2$
W_{102}	$\ddot{x}_d x$	W_{111}	$C_R(\alpha)$
W_{103}	$\ddot{x}_d x^2$	W_{112}	$T_c(\alpha) \left[\frac{V_J}{V_O}(\alpha) \right]^2 x$
W_{104}	\dot{x}	W_{113}	$C_R(\alpha)x$
W_{105}	$\dot{x}x$	W_{114}	$T_c(\alpha) \left[\frac{V_J}{V_O}(\alpha) \right]^2 x^2$
W_{106}	$\dot{x}x^2$	W_{115}	$C_R(\alpha)x^2$
W_{107}	x	W_{116}	$\dot{x}\dot{e}$
W_{108}	x^2	W_{117}	$\dot{x}e$
W_{109}	x^3	W_{118}	$xx\dot{e}$
		W_{119}	xxe

TABLE 4. PARAMETER ESTIMATION TERMS

No.	Terms	No.	Terms
$\hat{\Theta}_{101}$	$\hat{M}_s \frac{2\hat{C}_1^2}{\hat{C}_2 \hat{N}^2}$	$\hat{\Theta}_{110}$	$\hat{T}_{h1} \frac{2\hat{C}_1^2}{\hat{C}_2 \hat{N}^2}$
$\hat{\Theta}_{102}$	$\hat{M}_s \frac{4\hat{C}_1}{\hat{N}^2}$	$\hat{\Theta}_{111}$	$\hat{T}_{b1} \frac{2\hat{C}_1^2}{\hat{C}_2 \hat{N}^2}$
$\hat{\Theta}_{103}$	$\hat{M}_s \frac{2\hat{C}_2}{\hat{N}^2}$	$\hat{\Theta}_{112}$	$\hat{T}_{h1} \frac{4\hat{C}_1}{\hat{N}^2}$
$\hat{\Theta}_{104}$	$\hat{C}_s \frac{2\hat{C}_1^2}{\hat{C}_2 \hat{N}^2}$	$\hat{\Theta}_{113}$	$\hat{T}_{b1} \frac{4\hat{C}_1}{\hat{N}^2}$
$\hat{\Theta}_{105}$	$\hat{C}_s \frac{4\hat{C}_1}{\hat{N}^2}$	$\hat{\Theta}_{114}$	$\hat{T}_{h1} \frac{2\hat{C}_2}{\hat{N}^2}$
$\hat{\Theta}_{106}$	$\hat{C}_s \frac{2\hat{C}_2}{\hat{N}^2}$	$\hat{\Theta}_{115}$	$\hat{T}_{b1} \frac{2\hat{C}_2}{\hat{N}^2}$

$\hat{\Theta}_{107}$	$\hat{k}\hat{r}_g \frac{2\hat{C}_1^2}{\hat{C}_2 \hat{N}^2}$	$\hat{\Theta}_{116}$	$\hat{M}_s \frac{2\hat{C}_2}{\hat{N}^2}$
$\hat{\Theta}_{108}$	$\hat{k}\hat{r}_g \frac{4\hat{C}_1}{\hat{N}^2}$	$\hat{\Theta}_{117}$	$\hat{M}_s \frac{2\hat{C}_2}{\hat{N}^2}$
$\hat{\Theta}_{109}$	$\hat{k}\hat{r}_g \frac{2\hat{C}_2}{\hat{N}^2}$	$\hat{\Theta}_{118}$	$\hat{M}_s \frac{2\hat{C}_2}{\hat{N}^2}$
		$\hat{\Theta}_{119}$	$\hat{M}_s \frac{2\hat{C}_2}{\hat{N}^2}$

ACKNOWLEDGMENTS

This research is supported by Office of Naval Research, which we gratefully acknowledge. Thanks are in particular due to Mr. Anthony Seman and Dr. Stephen Mastro.

REFERENCES

- [1] Sarpkaya T., "Torque and Cavitation Characteristics of Butterfly Valves," *Journal of Applied Mechanics*, Vol. Dec. 1961, pp 511 – 518
- [2] Park J. Y. and Chung M. K., 2006. "Study on Hydrodynamic Torque of a Butterfly Valve" Technical Briefs, *Journal of Fluids Engineering*, Vol. 128, Jan, pp1-8
- [3] Nataraj C. and Mousavi P., 2009. "Nonlinear Analysis of Solenoid Actuators and Butterfly Valve Systems ," *14th International Ship Control Systems Symposium*, Ottawa, Canada, Sept., pp 1-8
- [4] Brauer J. R., 2007. *Magnetic Actuators and Sensors*, Wiley IEEE Press, New Jersey.
- [5] Leutwyier Z. and Dalton H., 2008. "A CFD Study of the Flow Field, Resultant Force, and Aerodynamic Torque on a Symmetric Disk Butterfly Valve in a Compressible Fluid," *Journal of Pressure Vessel Technology*, Vol. 130, May, pp 021302-1~10
- [6] Pomet J.B. and Praly L., 1992. "Adaptive Nonlinear Regulation: Estimation from the Lyapunov Equation," *IEEE Trans. on Automatic Control*, Vol.37, June, pp. 729-740
- [7] Pohl J., Sethson, M., Krus, P., and Palmberg, J-O., 2002. "Modeling and Simulation of a Fast 2/2 Switching Valve," *Proceedings of the Institution of mechanical engineers. Part I, Journal of systems and control engineering*, (216), 2, pp. 105-116
- [8] Krstic, M., Kanellakopoulos, I., and Kokotovic, P., 1995. *Nonlinear and Adaptive Control Design*, 1st ed., A Vol. of *Series on Adaptive and Learning Systems for Signal Processing*. John Wiley & Sons Inc., New York, NY.